

**NIST Electron Effective-Attenuation-Length Database**

Version 1.3

Users' Guide

---

Prepared by:

C. J. Powell, Surface and Microanalysis Science Division  
National Institute of Standards and Technology  
Gaithersburg, MD, USA

A. Jablonski, Institute of Physical Chemistry,  
Polish Academy of Sciences, Warsaw, Poland

January, 2011

**U.S. Department of Commerce**  
National Institute of Standards and Technology  
Standard Reference Data Program  
Gaithersburg, Maryland 20899

---

The National Institute of Standards and Technology (NIST) uses its best efforts to deliver a high quality copy of the database and to verify that the data contained therein have been selected on the basis of sound scientific judgment. However, NIST makes no warranties to that effect, and NIST shall not be liable for any damage that may result from errors or omissions in the database.

---

For a literature citation, the database should be viewed as a book published by NIST. The citation would therefore be:

C. J. Powell and A. Jablonski, *NIST Electron Effective-Attenuation-Length Database - Version 1.3*, National Institute of Standards and Technology, Gaithersburg, MD (2011).

---

©2011 copyright by the U.S. Secretary of Commerce on behalf of the United States of America. All rights reserved. No part of this database may be reproduced, stored in a retrieval system, or transmitted, in any form or by any means, electronic, mechanical, photocopying, recording, or otherwise, without the prior written permission of the distributor.

Certain trade names and other commercial designations are used in this work for the purpose of clarity. In no case does such identification imply endorsement by the National Institute of Standards and Technology nor does it imply that the products or services so identified are necessarily the best available for the purpose.

Microsoft, MS-DOS, Windows® 95, Windows® 98, Windows® NT, Windows® 2000, Windows® ME, Windows® XP, Windows® Vista, and Windows® 7 are registered trademarks of Microsoft Corporation.

## **ACKNOWLEDGMENTS**

The authors thank Ms. L. D. Decker for testing the database and for editorial assistance.

## TABLE OF CONTENTS

I. INTRODUCTION .....	1
II. GETTING STARTED .....	4
Packet Content .....	4
System Requirements .....	4
Installation .....	5
Removal of the Database .....	5
III. STRUCTURE OF THE PROGRAM .....	6
Main Menu .....	6
IV. RUNNING THE DATABASE PROGRAM .....	12
Starting the Database .....	12
Input Parameters (second option of the main menu) .....	12
Class of Material .....	12
Analyzed Electrons .....	12
IMFP and TMFP .....	13
Experimental Configuration .....	13
Database (first option of the main menu) .....	14
Effective Attenuation Length (EAL) .....	14
Emission Depth Distribution Function (DDF) .....	15
Correction Factor (CF) .....	16
File Management (third option of the main menu) .....	16
Save Created Files .....	16
Delete Files .....	17
Print Files .....	17
Print Figures .....	17
Load Files .....	18
Comparisons (fourth option of the main menu) .....	18
V. UNCERTAINTIES OF DATA .....	19
Uncertainties of EAL Data .....	19
Uncertainties of IMFP Data .....	20
Uncertainties of TMFP Data .....	22
Uncertainties of Transport Approximation .....	22
Uncertainties of DDF Data .....	23
Uncertainties of CF Data .....	23
VI. REFERENCES .....	24
APPENDIX A: VALUES OF ELECTRON BINDING ENERGIES AND OF THE PHOTOIONIZATION ASYMMETRY PARAMETER $\beta$ .....	26
APPENDIX B: PREDICTIVE FORMULAE FOR ELECTRON INELASTIC MEAN	

FREE PATH .....	31
TPP-2M Equation of Tanuma, Powell, and Penn .....	31
G-1 Equation of Gries .....	35
Atomic Weight and Density Data .....	35
APPENDIX C: DEFINITIONS OF ELECTRON EFFECTIVE ATTENUATION LENGTHS...	37
Local EALs .....	37
Practical EALs .....	37
Average Practical EAL .....	38
EAL for Quantitative Analysis .....	38
APPENDIX D: CUMPSON AND SEAH PREDICTIVE FORMULA FOR ELECTRON EFFECTIVE ATTENUATION LENGTHS .....	39
APPENDIX E: OTHER PREDICTIVE FORMULAE FOR ELECTRON EFFECTIVE ATTENUATION LENGTHS .....	40
APPENDIX F: CONTACTS .....	41

## I. INTRODUCTION

This database provides values of electron effective attenuation lengths (EALs) in solid elements and compounds at selected electron energies between 50 eV and 2,000 eV.

The database was designed mainly to provide EALs for applications in surface analysis by Auger-electron spectroscopy (AES) and X-ray photoelectron spectroscopy (XPS). For these applications, EALs are needed mainly for measurements of the thicknesses of overlayer films and to a much lesser extent for measurements of the depths of thin marker layers (so-called  $\delta$ -layers).

The formal definitions of EALs for measurement of overlayer-film thicknesses and marker-layer depths are different, as described elsewhere [1]. In addition, it is possible to define "local" EALs, useful for a small range of thicknesses or depths, and "practical" EALs, useful for thicknesses or depths likely to be of practical relevance [1]. While the database can provide both local and practical EALs for measurements of overlayer-film thicknesses and of marker-layer depths, the practical EALs for measurement of overlayer-film thicknesses will likely be of greatest interest for most AES and XPS applications. These practical EALs can differ from the corresponding electron inelastic mean free paths (IMFPs) by up to about 35 % for common AES and XPS measurement conditions due to the effects of elastic-electron scattering.

The EALs (and other functions and parameters listed below) are calculated from analytical expressions derived from solution of the kinetic Boltzmann equation within the transport approximation [2]. Examples of EALs obtained by this approach are described in several publications [3-6]. The EALs depend on two material-dependent parameters, the IMFP and the transport mean free path (TMFP). IMFPs are obtained from the NIST Electron Inelastic-Mean-Free-Path Database [7] and TMFPs are obtained from elemental TMFPs in the NIST Electron Elastic-Scattering Cross-Section Database [8,16] and, for compounds, the weighted TMFPs for the constituent elements [9]. In addition, the EALs for XPS depend on the photoionization asymmetry parameter; suitable values of this parameter for XPS with characteristic Mg and Al  $K\alpha$  x-rays are given in Appendix A.

The user will first specify values for certain initial parameters (including the material of interest (element, inorganic compound, or organic compound), the electron energy, the photoionization asymmetry parameter (for XPS), a particular source of IMFP data from the NIST IMFP Database, and the experimental configuration). The user can then choose to obtain local or practical EALs, and will then typically generate a Table of EAL values for selected overlayer-film thicknesses or marker-layer depths; these EAL values can be stored, if desired, for further analysis. The EALs are then displayed on the screen as a function of film thickness or marker depth, and compared with the IMFP. By clicking on the screen, a user can select a particular thickness or depth of interest, and the EAL for that thickness or depth will be displayed together with the percentage attenuation of an assumed substrate-electron signal (for an overlayer) or the percentage attenuation of the marker-layer signal will be displayed for the selected thickness or depth, respectively.

As just indicated, the EAL is typically a function of overlayer thickness (or marker-layer depth). For emission angles less than about  $60^\circ$  (with respect to the surface normal) and for overlayer-film thicknesses of practical relevance in AES and XPS measurements, however, the practical EAL does not vary appreciably with overlayer thickness or emission angle [3-6,10]. The database can provide an average practical EAL for a selected film thickness (or marker depth) at the specified emission angle. This average practical EAL can be used as the “lambda parameter” in measurements of overlayer-film thicknesses by AES and XPS [1, 3-6]. For emission angles larger than about  $60^\circ$ , it will often be necessary to obtain a practical EAL for an estimated overlayer-film thickness so that a more accurate film thickness can be determined by iteration.

The database also can supply values of certain other parameters for an infinitely thick material: the electron mean escape depth [11], the EAL for quantitative analysis by AES and XPS [1], the correction parameters  $Q_x$  and  $\beta_{\text{eff}}$  for XPS [12,13], and the correction parameter  $Q_A$  for AES [12,13]. In addition, the database supplies the average EAL for elemental solids from the CS2 EAL estimation formula proposed by Cumpson and Seah, as described in Appendix D [10]. Appendix E gives information on two other analytical formulae that are useful for estimating average EAL values.

The database has two further options. First, the user can obtain values of the emission depth distribution function (DDF) for a specified material and electron energy. This DDF can be visually compared with the DDF obtained when elastic-electron scattering was neglected. Second, the user can obtain values of the correction factor (CF), the ratio of the DDF with elastic-electron scattering considered to the DDF with elastic-electron scattering neglected [14]. For each of these options, Tables of the DDF and the CF are created and can be stored for later analysis.

EAL, DDF, or CF data stored in files can be printed and saved to other directories. It is also possible to make on-screen comparisons of EAL, DDF, or CF data in selected files. These graphical comparisons can be printed and saved in Windows bitmap format for easy incorporation into other documents.

NIST released Version 1.0 of the Electron Effective-Attenuation Length Database (SRD 82) in 2001. This version included transport cross sections obtained from Version 2.0 of the NIST Electron Elastic-Scattering Cross-Section Database [8]. These transport cross sections had been obtained from differential elastic-scattering cross sections that were calculated using the Thomas-Fermi-Dirac potential to describe the interaction between an electron and an atom [15].

Version 3.1 of the NIST Electron Elastic-Scattering Cross-Section Database was released in 2003 [16]. This database contains differential elastic-scattering cross sections and transport cross sections that were calculated from a relativistic Dirac partial-wave analysis in which the potentials were obtained from Dirac-Hartree-Fock electron densities computed self-consistently for free atoms [15]. This potential is believed to be more reliable than the Thomas-Fermi-Dirac potential used previously [15]. Version 1.1 of the Electron Effective-Attenuation-Length Database contains transport cross sections from Version 3.1 of the Electron Elastic-Scattering Cross-Section Database [16] instead of those from Version 2.0 of this database [8]. The new transport cross sections are considered to be more reliable than those used earlier [15].

Version 1.2 of the Electron Effective-Attenuation-Length Database was released in December, 2009. This version corrects bugs in the software used to calculate the mean escape depth and the effective attenuation length for quantitative analysis. The opportunity was also taken to update some references and to include some more recent references.

Version 1.3 of the Electron Effective-Attenuation-Length Database was released in January, 2011. The installation program for Version 1.3 was changed so that it would operate on newer versions of the Windows operating system. There were no changes or additions to the data in the database although a new About box was added to the main menu. This box shows three references, a 2002 critical review [1], a 2002 paper [17] that presents comparisons of practical effective attenuation lengths for XPS which were obtained from different algorithms, and a 2009 review [18] that discusses evaluations of the compiled data, methods of determination, and uncertainty.

Further information on the use of effective attenuation lengths in quantitative applications of XPS and the effects of surface roughness can be found in a 2010 review [52].



## II. GETTING STARTED

### Packet Content

CD-ROM  
Users' guide

Alternatively, the files on the CD-ROM and a PDF file with the Users' Guide can be downloaded from NIST (<http://www.nist.gov/srd/surface.cfm>).

### System Requirements

1. Personal computer with Windows 95, Windows 98, Windows NT, Windows 2000, Windows ME, Windows XP, Windows Vista, or Windows 7 operating system
2. CD-ROM drive
3. Screen resolution: 1024 by 768 pixels.
4. System font size: small fonts.
5. Printer: Laser printer supporting the PCL 6 printer language.
6. Hard disk space of at least 7.3 MB. Larger amounts of storage are required if numerous files are created with the database. It is suggested that 15 Megabytes be available, particularly if graphic files are created.

The database has been designed to operate optimally at the screen resolution given above. However, it can also be operated at a lower screen resolution, e.g., 640 by 480 pixels, or 800 by 600 pixels. At higher resolutions, the database will operate correctly but there may be difficulty in reading text on the screen. For all resolutions, small system fonts must be selected.

To change the screen resolution or the system font size, follow these steps:

1. Double click the **My Computer** icon on the desktop.
2. Click the **Control panel** icon.
3. Double click the **Display** icon.
4. Click on the **Settings** tab.
5. Set a given resolution by moving the slider.

To change the system font size, proceed as follows depending on the operating system in use:

For Windows 95 or NT, select **Small Fonts** in the **Font Size** box.

For Windows 98, click on the **Advanced...** button, select the **General** tab, and then select the **Small Fonts** option in the **Display** box.

For Windows XP, click on the **Advanced...** button, and then select the **Normal size (96 DPI)** option in the **Display** box.

For Windows Vista, click on **Appearance and Personalization**, **Personalization**, **Adjust font size (DPI)** in the left pane, and select **Default scale (96 DPI)**.

For Windows 7, click on **Appearance and Personalization, Display**, and select **Small - 100 %** (default option).

## **Installation**

1. Insert the CD-ROM into the disk drive of the computer.
2. Click the **Start** button on the task bar.
3. Click the **Run** command.
4. Type D:\SETUP (if D: is the drive letter for the disk drive) and click OK.
5. Follow instructions on the screen.

Alternatively, the following procedure can be used:

1. Insert the disk into the disk drive of the computer.
2. Double-click **My Computer** on the desktop.
3. Double-click the icon corresponding to the disk drive.
4. Double-click the **Setup** icon (showing the computer).
5. Follow instructions on the screen.

If files have been downloaded into a directory on the user's personal computer, double-click the **Setup** icon (i.e., **setup.exe**).

Should difficulty be encountered in installing the database as described above (e.g., due to security settings on the computer), the database can be launched by double-clicking on **EAL13.exe** located in the Program Files directory.

By default, the database is installed in the directory C:\PROGRAM FILES\NIST\EAL13. Furthermore, an EAL13 icon is created. This icon appears after clicking the **Start** button and choosing **Programs**.

## **Removal of the Database**

1. Double click **My Computer** on the desktop.
2. Double click the **Control panel** icon.
3. Double click the **Add/Remove Programs** icon.
4. Select **Install/Uninstall**.
5. In the list of programs, click **EAL13**.
6. Click the button **Add/Remove**.

### III. STRUCTURE OF THE PROGRAM

#### Main Menu

The six options of the Main Menu are listed in the upper part of the title screen (Fig. 1), and the submenus corresponding to the first four options are shown in Figs. 2 to 5. The functions of the six main menu options are briefly described here; further information is given in Section IV.

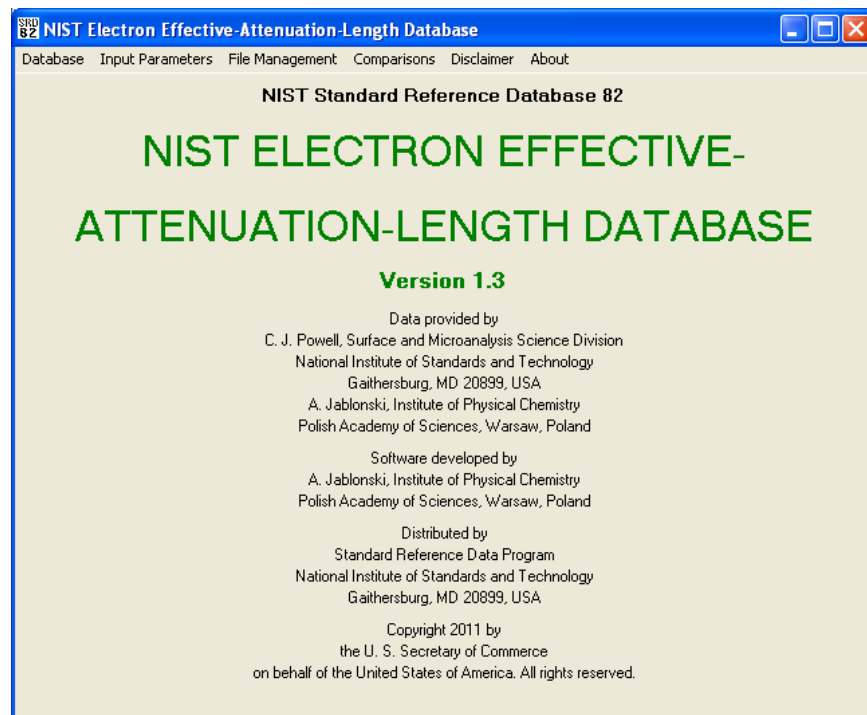


Fig. 1. The title screen and main menu.

1. Database (Fig. 2)

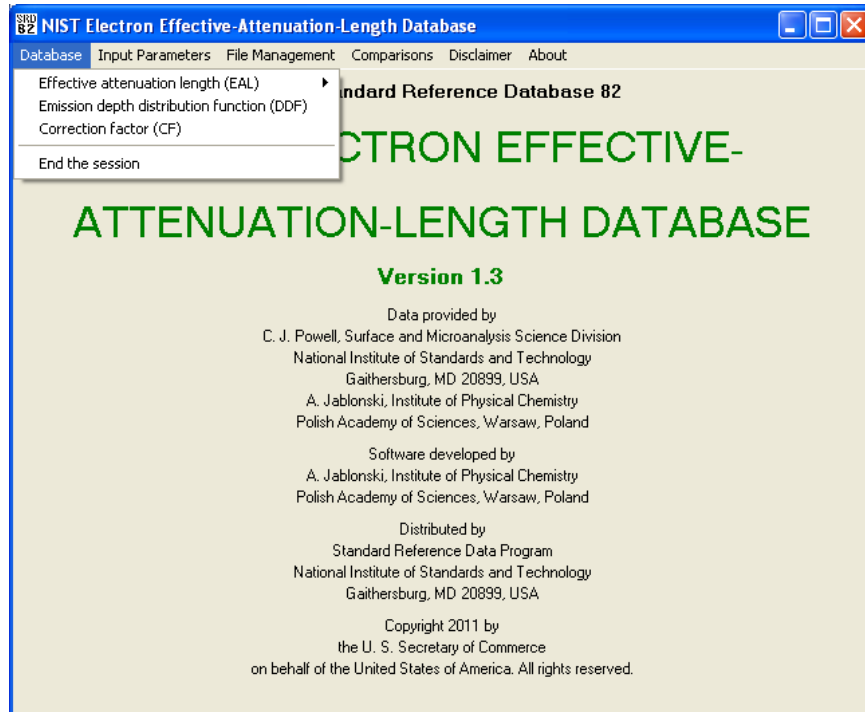


Fig. 2(a). First option of the main menu (Database).

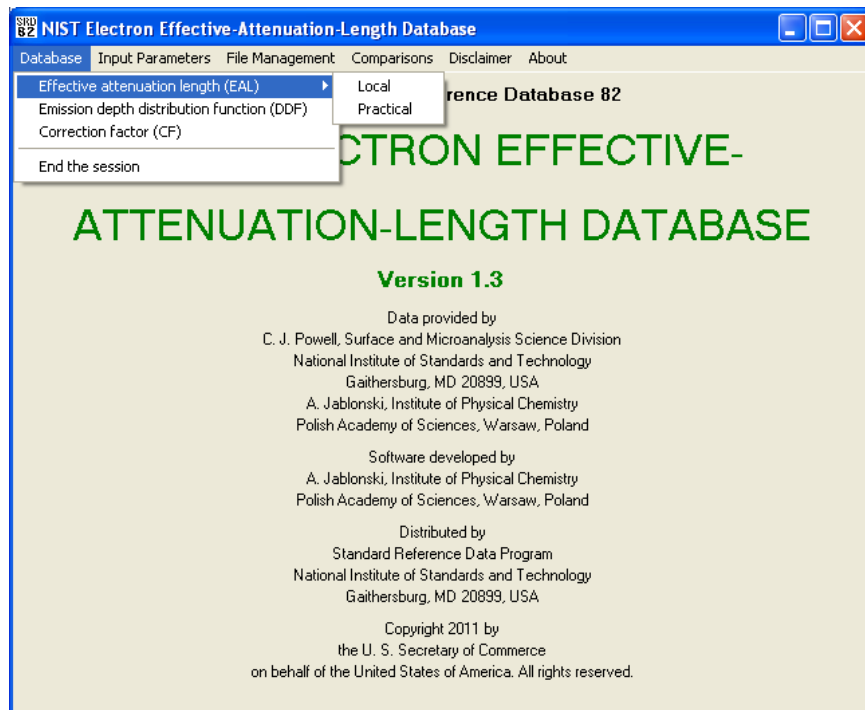


Fig. 2(b). First option of the main menu (Database) and submenu for Effective attenuation length (EAL).

With this option, the user can obtain local and practical effective attenuation lengths (EALs), the emission depth distribution function (DDF), and the correction factor (CF) for a DDF obtained by neglecting the effects of elastic-electron scattering. These options are grayed out until after the user has entered appropriate input parameters. Operation of the database can be terminated by choosing End the session.

## 2. Input Parameters (Fig. 3)

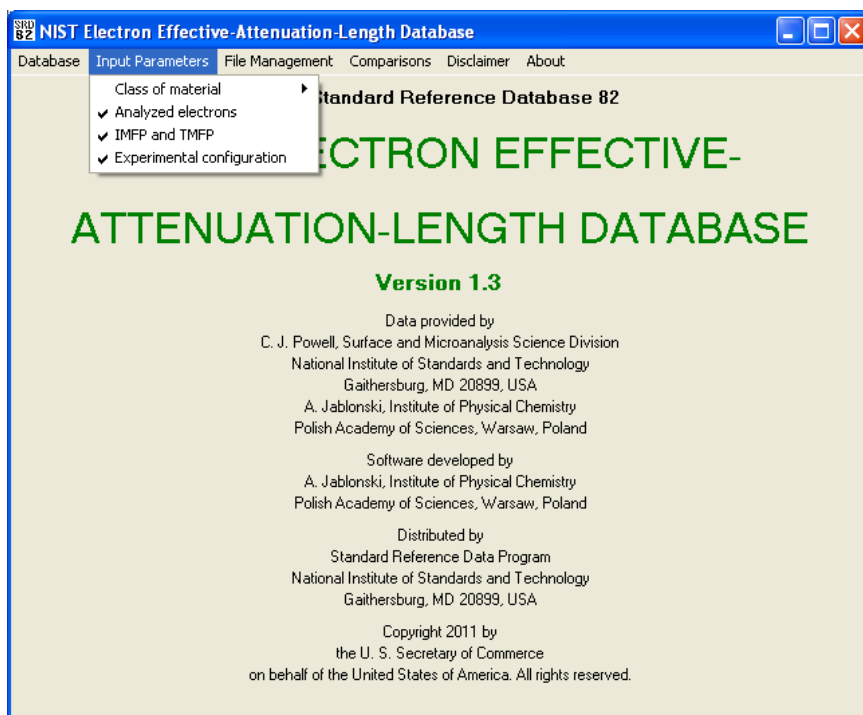


Fig. 3(a). Second option of the main menu (Input Parameters).

The user specifies here the class of material (element, inorganic compound, or organic compound), information concerning the analyzed electrons (XPS or AES, whether data for the inelastic mean free path (IMFP) and the transport mean free path (TMFP) are to be obtained from the database or supplied by the user, the electron energy, and (for XPS) the asymmetry parameter), specific source of IMFP data from the database to be used and the units for IMFPs and TMFPs, and the experimental configuration.

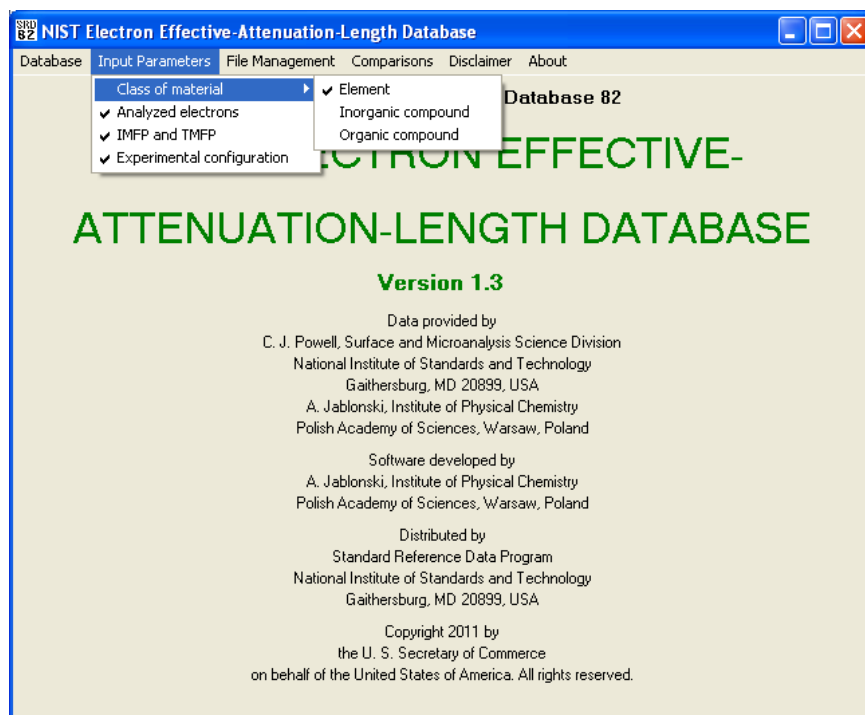


Fig. 3(b). Second option of the main menu (Input Parameters) with submenu for Class of material.

### 3. File Management (Fig. 4)

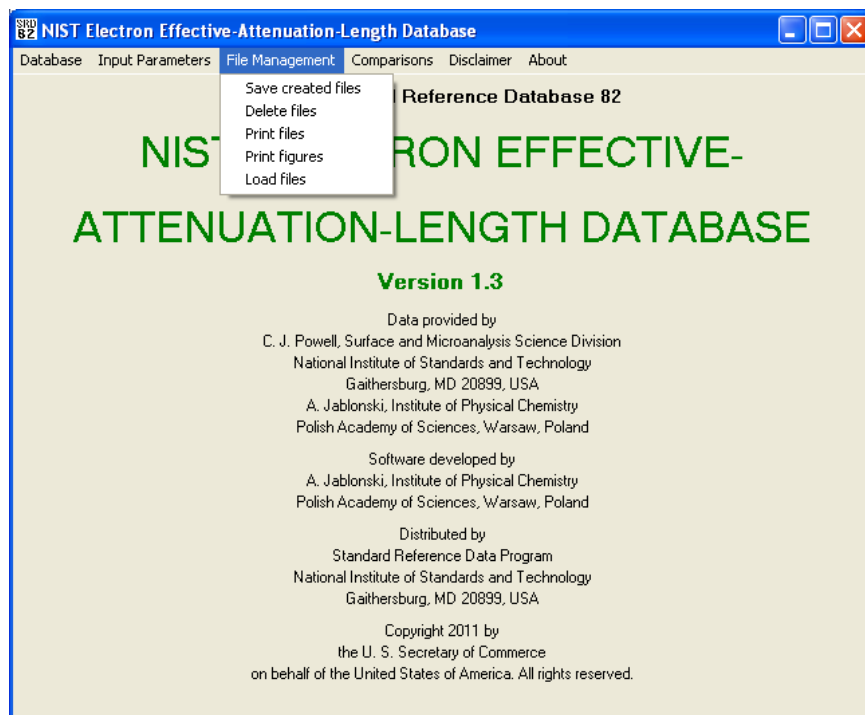


Fig. 4. Third option of the main menu (File Management).

This option allows the user to save files created in the present session to another directory for permanent storage, to delete files from the database directory, to print files, to print figures, and to load files that were created in earlier sessions and stored in another directory.

#### 4. Comparisons (Fig. 5)

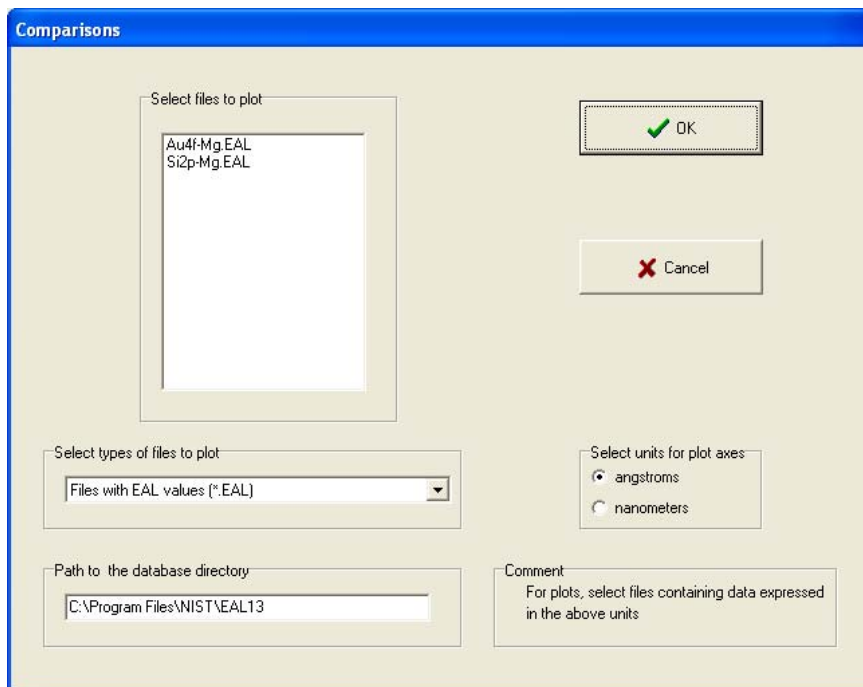


Fig. 5. Example of screen that appears when the Fourth option of the main menu (Comparisons) is selected

With this option, EAL, DDF, and CF data as a function of thickness or depth for different materials and/or different experimental configurations can be graphically compared.

#### 5. Disclaimer (Fig. 6)

The NIST disclaimer is stated.

#### 6. About box (Fig. 7)

The About box gives information on the release date of this version of the database, how the database should be cited in publications, and references to evaluations of the compiled data, methods of determination, and uncertainties [1,17,18].

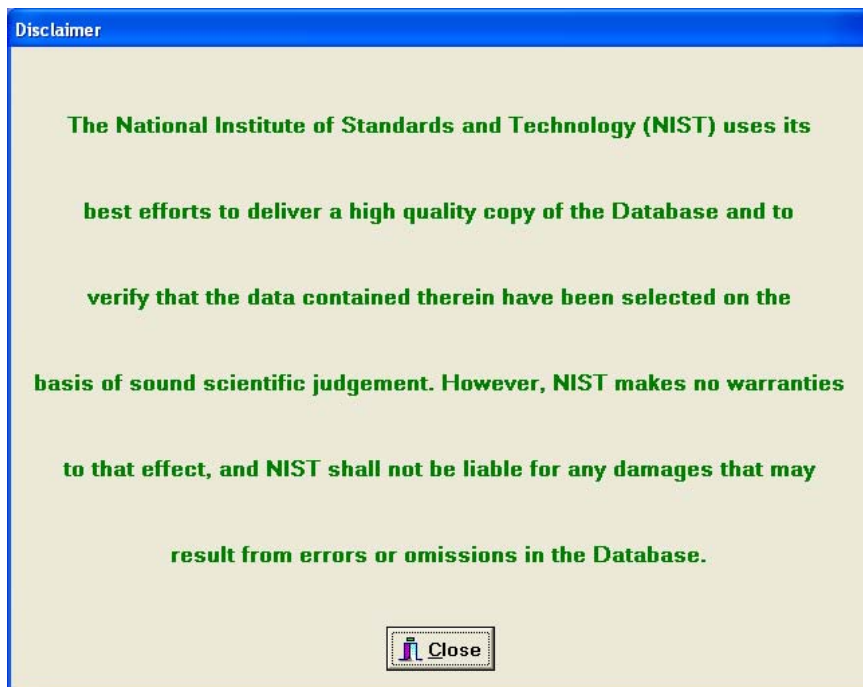


Fig. 6. NIST disclaimer.

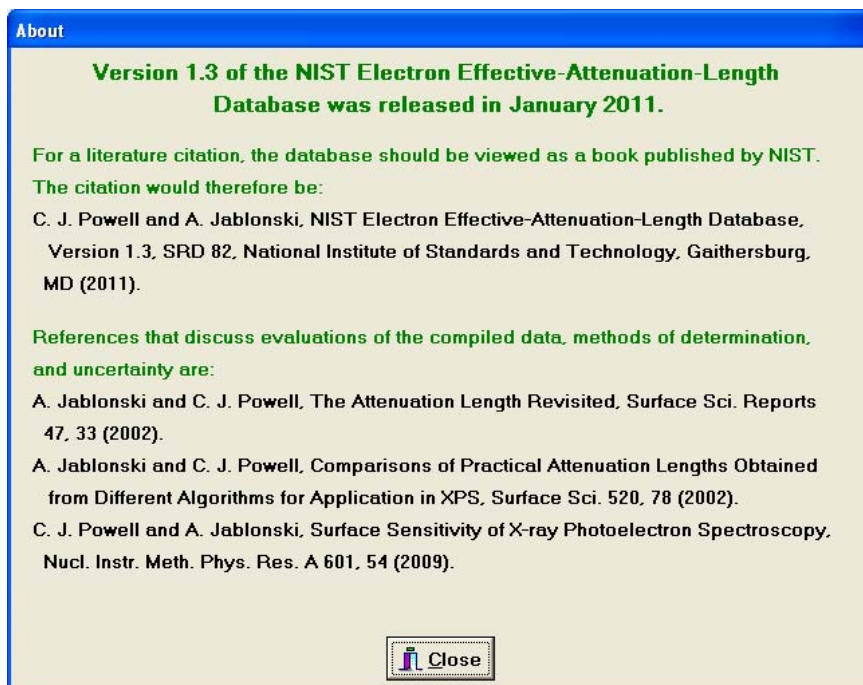


Fig. 7. The About box.



## IV. RUNNING THE DATABASE PROGRAM

### Starting the Database

The database can be started by any of the following means:

1. Click the Start button, choose Programs, and then the **EAL13** icon.
2. Click the Start button, choose Run, and type:  
C:\PROGRA~1\NIST\EAL13\EAL13,  
and then click **OK**.
3. Double-click the **My Computer** icon on the desktop, select the  
C:\PROGRAM FILES\NIST\EAL13 directory, and double-click on the **EAL13** icon.

The user will normally start with the **Input Parameters** option on the main menu and then proceed to the **Database** option on the main menu to obtain effective attenuation lengths, an emission depth distribution function, or the correction factor for the application of interest. After files have been created by the database, the various **File Management** options and the **Comparisons** option on the main menu can be utilized.

### Input Parameters

(Second option of the main menu)

#### Class of Material

(First option of the Input Parameters option on the main menu)

The user can select Element, Inorganic compound, or Organic compound (Fig. 3(b)). If Element is chosen, a Periodic Table of the elements will appear. The user should click on the element of interest and then the **OK** button. If Inorganic compound or Organic compound is chosen, a Periodic Table will appear and the user should click on the elements present in the compound, and then click the **OK** button.

#### Analyzed Electrons

(Second option of the Input Parameters option on the main menu)

The user will select the technique of interest (AES or XPS), the source of inelastic mean free path (IMFP) and transport mean free path (TMFP) values (database or user-provided values), the relevant electron kinetic energy with respect to the Fermi level (between 50 eV and 2000 eV), and (for XPS) the value of the appropriate photoionization asymmetry parameter  $\beta$  (Fig. 3(a)). Values of core-electron binding energies and of  $\beta$  are given in Appendix A for the more intense photoelectron lines observed with Mg and Al  $K\alpha$  x-rays. Photoelectron kinetic energies can be simply determined from the relevant binding energies and the particular x-ray energy.

## **IMFP and TMFP**

### **(Third option of the Input Parameters option on the main menu)**

If the user had previously chosen to obtain data for an element, a screen will appear on which the user will select the source of IMFP data to be employed in the following calculations. For elements for which calculated IMFPs or IMFPs measured by elastic-peak electron spectroscopy (EPES) are available [19,20], the user can select a source of data. For other elements, the user can select to have IMFPs derived from the TPP-2M predictive IMFP formula of Tanuma *et al.* [21] or the G-1 predictive IMFP formula of Gries [22]. A choice also needs to be made of the IMFP units (angstroms or nanometers).

If the user had previously chosen to obtain data for an inorganic compound or organic compound, a screen will appear on which the user will enter the name of the compound and the stoichiometry coefficients for the previously selected elements in the compound. A choice needs to be made of the units for the IMFP, TMFP, and EAL (angstroms or nanometers), and the predictive equation from which IMFPs will be calculated (the TPP-2M equation of Tanuma *et al.* [21] or the G-1 equation of Gries [22]). The user then enters the density of the compound and, for the TPP-2M equation, the number of valence electrons per molecule and the bandgap energy; information on the latter two parameters is given in Appendix B.

If the user had previously chosen to provide IMFP and TMFP values for an element, a screen will appear on which the user can enter the name of the element (the elemental symbol is shown as a default), the IMFP, the TMFP, and the density (a default value of the density is provided). The appropriate IMFP and TMFP units should also be selected (angstroms or nanometers).

## **Experimental Configuration**

### **(Fourth option of the Input Parameters option on the main menu)**

A screen will appear on which the user will specify the experimental configuration. For XPS, the user will specify the direction of x-rays from the x-ray source onto the specimen material. The angle of x-ray incidence (designated as  $\theta$  on this and later screens) can be increased or decreased in increments of  $1^\circ$  or  $10^\circ$ . For both AES and XPS, the user will specify the angle of electron emission (designated as  $\alpha$  on this and later screens) to the analyzer in the same way. For XPS, the adjustments for  $\theta$  and  $\alpha$  are made by clicking on either **X-ray source** or **Analyzer** in the box at the top-left of the screen. For XPS, it is assumed that the plane of x-ray incidence is coplanar with the plane of electron emission.

## Database

(First option of the main menu)

### Effective Attenuation Length (EAL)

(First option of the Database option on the main menu)

The user will first select “Local” or “Practical” from the submenu for this option to give local or practical EALs as desired (Fig. 2(b)) [1]. For most AES and XPS applications, the practical EAL option should be selected.

On the following screen, the user can choose to obtain EALs from the overlayer-film thickness definition (the default choice) or the marker-layer depth definition [1]. For most AES and XPS applications, the overlayer-film thickness definition will be appropriate. Appendix C contains the defining equations for local and practical EALs for the overlayer-film thickness and marker-layer depth applications. Reference 1 should be consulted for further guidance on the rationale for these different definitions; references 3-6 contain examples of EALs from these different defining equations for various materials and different experimental configurations.

In the **Create table** box on the right side of the screen, the user will specify both the number of EAL values desired and the maximum overlayer thickness (or marker depth) of interest. On clicking the **Calculate** button, a Table of EAL values will then be displayed showing EALs for thicknesses (or depths) up to the maximum value previously entered. The user can, if desired, create a file by entering a suitable file name in the **Create file** box at the bottom right of the screen, and then clicking the **Create** button. Such a file will be given the .EAL extension. A window will then appear on the screen indicating that the file has been successfully created; this window would show a diagnostic if, for example, an unsuitable file name had been chosen. This option is a convenient means of storing EALs for later analysis.

On clicking the **Next** button, a screen will appear with a display of EAL values from the previous Table as a function of thickness (or depth); the corresponding IMFP is also displayed for comparison. By clicking on the screen in the vicinity of a thickness or depth of interest, a red cursor will appear and the EAL for that thickness or depth will be shown in a box on the right side of the screen. The position of the cursor can be adjusted (in intervals of 1 angstrom or 10 angstroms) by selecting one of the **Change thickness/depth** options on the right side of the screen and by clicking on one of the two buttons at the bottom of the screen. Another box on the right side of the screen will display the percentage attenuation of an assumed substrate signal (for the overlayer-film definition of the EAL) or of a marker layer (for the marker-layer definition of the EAL). If desired, the display to the left of the cursor can be magnified to fill the screen by clicking on the **Enlarge** button; the original display can be obtained by clicking on the **Reset** button.

For the practical EAL option, the user can click on the **Average practical EAL** button (after selecting a thickness or depth of interest on the display) and a screen will appear with a summary of the EAL calculations for the selected conditions. The box at the top left of this screen will show the practical EAL from the previous screen for the indicated thickness or depth together

with the percentage signal attenuation. This box will also show the average practical EAL for thicknesses (or depths) from zero to the selected thickness (or depth).

The middle-left box on this screen contains values of related parameters (for an infinitely thick material) that may be of interest for other applications. Values are given here of the electron mean escape depth [11], the EAL for quantitative analysis by AES and XPS [1], the correction parameters  $Q_x$  and  $\beta_{\text{eff}}$  for XPS [12,13], and the correction parameter  $Q_A$  for AES [12,13]. The correction parameters  $Q_x$  and  $Q_A$  describe the reduced yield of photoelectrons and Auger electrons, respectively, due to elastic-electron scattering. The correction parameter  $\beta_{\text{eff}}$  is an effective photoionization asymmetry parameter for XPS that is different from  $\beta$  due to the effects of elastic-electron scattering.

The bottom-left box on this screen provides the average EAL for elemental solids from the CS2 EAL estimation formula proposed by Cumpson and Seah [10]. Although these authors reported EALs from the CS2 equation for two compounds, details of how the equation should be evaluated for compounds have not been published [10]. Further information on the CS2 equation is given in Appendix D.

The user can create a file with the information on this screen by entering a suitable name in the Create file box in the middle-right of the screen, and clicking on the **Create** button. This file will be given the .AVE extension.

Finally, the user can return to the previous screen, if desired, by clicking on the **Return** button so that, for example, average EALs can be obtained for other thicknesses or depths.

### **Emission Depth Distribution Function (DDF) (Second option of the Database option on the main menu)**

With this option, the user can obtain values of the emission depth distribution function (DDF) for the previously selected material and electron energy (Fig. 2(a)). The DDF can be calculated without normalization (the default choice) or with two choices of normalization [11] in the box near the bottom of the screen. If desired, the DDF can be normalized so that it is equal to unity at the surface or the integral of the DDF can be made equal to unity.

In the **Create table** box on the right side of the screen, the user will specify both the number of DDF values desired and the maximum depth of interest. On clicking the **Calculate** button, a Table of DDF values will then be displayed showing DDFs for depths up to the maximum value previously entered. The user can, if desired, create a file by entering a suitable file name in the **Create file** box at the bottom right of the screen, and then clicking the **Create** button. Such a file will be given the .DDF extension. This option is a convenient means of storing DDFs for later analysis.

On clicking the **Plot** button, a screen will appear with a display of DDF values from the previous Table as a function of depth; this is the line designated DDF TA (where TA refers to calculation from the transport approximation). This screen also shows a line designated DDF SLA, which refers to the DDF from the so-called straight-line approximation in which elastic scattering of the

signal electrons, is neglected. The DDF TA line can thus be visually compared with the DDF SLA line. These DDFs can be displayed in either logarithmic or linear coordinates by clicking on the appropriate button in the Change coordinates box.

By clicking on the screen in the vicinity of a depth of interest, a red cursor will appear and the DDF for that depth will be shown in a box on the right side of the screen. The position of the cursor can be adjusted (in intervals of 1 angstrom or 10 angstroms) by selecting one of the **Change depth** options on the right side of the screen and by clicking on one of the two buttons at the bottom of the screen. If desired, the display to the left of the cursor can be magnified to fill the screen by clicking on the **Enlarge** button; the original display can be obtained by clicking on the **Reset** button.

### **Correction Factor (CF)**

**(Third option of the Database option on the main menu)**

With this option, the user can obtain values of the correction factor (CF) for the previously selected material and electron energy (Fig. 2(a)). The CF is the ratio of the DDF with elastic-electron scattering considered to the DDF with elastic-electron scattering neglected [14]. Values of CF can be calculated and displayed as described for the DDF in the previous section. In the display of CF values, the line designated CF TA represents the CF obtained from the transport approximation while the horizontal line designated CF SLA (at unity) represents the CF from the straight-line approximation (for which elastic-electron scattering is neglected). Files can be created with CF values, and these will be given the .CFF extension.

### **File Management**

**(Third option of the main menu)**

With this option, a user can save files created in the present session to another directory for permanent storage, delete files from the database directory, print files containing EAL, DDF, or CF data, print figures (from files generated with the Comparisons option on the main menu), and load files containing data or figures that were created in earlier sessions and stored in another directory (Fig. 4). These options will be described briefly in turn.

### **Save Created Files**

**(First option of the File Management option on the main menu)**

Files containing EAL, DDF, or CF values are created by the database (as described above) as text files in the directory in which the database is located (C:\PROGRAM FILES\NIST\EAL is the default directory); these files are created with .EAL, .DDF, or .CFF extensions, respectively. Files containing a summary of EAL data have the .EAL extension and files with figures have the .BMP extension.

The Save files option allows the user to save selected files in the database directory to any other directory for permanent storage. If desired, files with particular extensions can be selected for display. The file(s) to be saved should be selected by clicking on the file name(s) (and simultaneously pressing the Shift key or the Ctrl key if multiple selections are desired). The

destination directory for the saved files is selected in the panel located in the lower-left corner of the screen. The user can then select one of the three buttons in the lower-right corner of the screen to indicate whether the selected files should be retained in the database directory after the Save files operation (the default option), whether these files should be removed from this directory, or whether all data files in the directory should be removed. The **OK** button should then be clicked to save the designated files.

### **Delete Files**

**(Second option of the File Management option on the main menu)**

Data files created during the present session or during previous sessions can be deleted with this option. It is possible to display files with selected extensions using the middle box on the left of the screen. The user then selects one or more files for deletion from the list. If desired, all data files in the database directory can be deleted by choosing the second button in the lower right of the screen. Deletion of the selected files occurs after the **OK** button is clicked.

### **Print Files**

**(Third option of the File Management option on the main menu)**

Data files created by the database (i.e., those with .EAL, .DDF, .CFF, and .AVE extensions) are text files and can be opened and printed by common word-processing software. These files can also be printed with this option of the database. If desired, the user can select files with a particular extension for listing. Unlike the previous file-management options, the user can only select a single file for printing at a time. Printing is initiated by clicking the **Print** button. If a user wishes to print files stored in other directories, these files can be loaded into the database directory using the Load files option described below.

### **Print Figures**

**(Fourth option of the File Management option on the main menu)**

Files with figures created by the Comparisons option of the database (see below) have the .BMP extension and can be inserted into documents produced by common word-processing software. These files can also be printed with this option of the database. A file can be selected and, after clicking the **Load image** button, the figure appears in the center of the screen. This figure can be printed in one of eight sizes by moving the pointer in the lower part of the screen with the mouse. The printed sizes are approximately 5 cm x 4 cm, 7 cm x 5 cm, 8.5 cm x 6.5 cm, 10 cm x 7.5 cm, 11.5 cm x 9 cm, 13 cm x 10 cm, 14.5 cm x 11 cm, and 16 cm x 12 cm for pointer positions 1, 2, 3, 4, 5, 6, 7, and 8, respectively. Clicking the **Print** button initiates printing. Files with figures that are stored in other directories can be loaded into the database directory using the Load files option.

## **Load Files**

**(Fifth option of the File Management option on the main menu)**

With this option, it is possible to transfer files to the current database directory (default: C:\PROGRAM FILES\NIST\EAL) that had been saved previously to other directories. It is possible to load files with the .EAL, .DDF, .CFF, .AVE, and .BMP extensions, and listings of files with selected extensions can be chosen using the box in the lower-right side of the screen. One or more of the files listed in the upper part of the screen can be selected and then loaded into the database directory by clicking **OK**.

## **Comparisons**

**(Fourth option of the main menu)**

This option is useful for making graphical comparisons of EAL, DDF, or CF data for the same material with different conditions (e.g., different experimental configurations, different electron energies, or different sources of IMFP or TMFP data) or for comparing such data for different materials (Fig. 5). The option is also useful for creating a graphical display with a single set of EAL, DDF, or CF data. These graphical displays can be stored or printed for later use.

It is necessary first to select the type of files for plotting, that is, files with the .EAL (the default option), .DDF, or .CFF extension. Up to four files can be selected at a time for comparison. It is important that the user select the appropriate units for the thickness or depth scales (angstroms or nanometers); this choice of unit must be the same as that made when the file was created. Particular care should be taken not to make comparisons of data from files that were created with different thickness or depth units.

After clicking the **OK** button, a graphical display of the selected files will appear. An example of such a comparison plot is shown in Fig. 7. In this example, practical EALs are shown for Si  $2p_{3/2}$  photoelectrons in Si and Au  $4f_{7/2}$  photoelectrons in Au (with excitation by Mg  $K\alpha$  x-rays at an incidence angle of  $54^\circ$  and for a photoelectron emission angle of  $0^\circ$  with respect to the surface normal) as a function of overlayer-film thickness. The display can be printed. In addition, a file can be created (with .BMP extension) so that the display can be incorporated into other documents using common word-processing software. The displays of DDF or CF data can be presented in either linear or logarithmic coordinates.

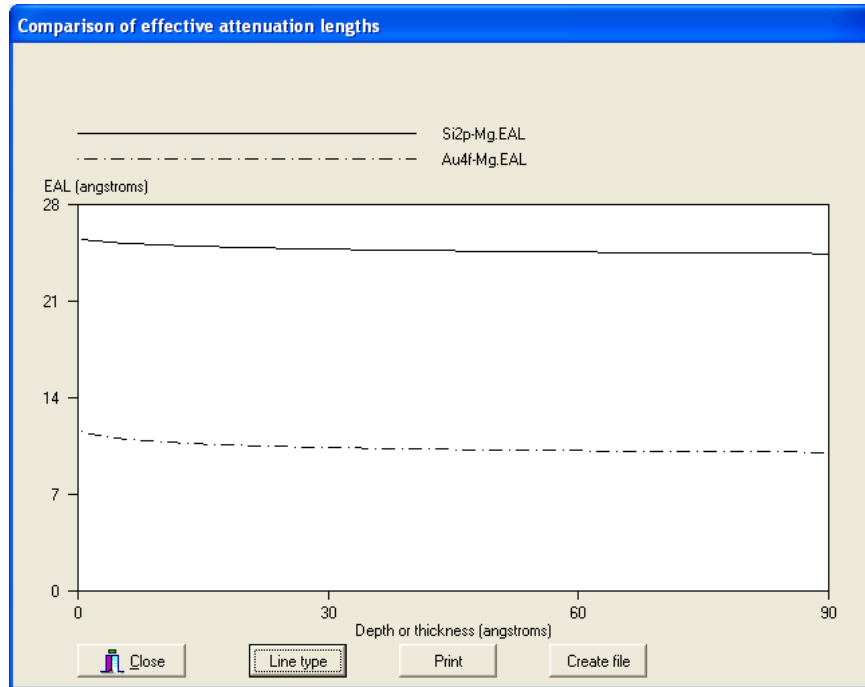


Fig. 7. Example of a comparison of practical EALs for Si 2p<sub>3/2</sub> photoelectrons in Si (solid line) and for Au 4f<sub>7/2</sub> photoelectrons in Au (dot-dashed line) for XPS with Mg K $\alpha$  x-rays at an incidence angle of 54° and for photoelectrons emitted at 0° with respect to the surface normal.

## V. UNCERTAINTIES OF DATA

We comment in turn on the uncertainties of EAL, DDF, and CF data from the database.

### Uncertainties of EAL Data

The uncertainties of the EAL values depend mainly on the uncertainties of the IMFP and TMFP data used in the calculations as well as on the uncertainty associated with use of the transport approximation [18]. The EAL calculation for the overlayer-film definition is based on the implicit assumption that the film is on a substrate with similar electron-scattering properties (i.e., similar values of the IMFP and TMFP). A Monte Carlo simulation of the attenuation of Si 2p photoelectrons in overlayer films of HfO<sub>2</sub> showed differences of up to 10 % in the derived EALs (compared to EALs obtained from the transport approximation) for film thicknesses less than an IMFP in the HfO<sub>2</sub> [29]. In this example, the electron-scattering properties of HfO<sub>2</sub> are substantially different from those of Si [29]. Further information on this topic is given in a recent review [18].

There are additional potential uncertainties associated with the neglect of surface roughness, surface-electronic excitations, and surface refraction [18,52]. It is difficult to assess the magnitude of these latter uncertainties with current scientific knowledge although it is thought that they should be smaller than other uncertainties (except, perhaps, for the effects of surface-



electronic excitations under near-grazing emission conditions for atomically smooth surfaces and for the effects of surface refraction for electron energies less than about 200 eV) [18,52].

### Uncertainties of IMFP Data

The uncertainties of IMFPs calculated from experimental optical data and of IMFPs measured by elastic-peak electron spectroscopy have been analyzed elsewhere [18-20]. The most detailed analysis was made for a group of seven solid elements for which there were at least two independent sources of calculated IMFPs and at least two independent sources of measured IMFPs. This analysis indicated that, for the calculated IMFPs, the average root-mean-square deviation *RMS* of the individual IMFPs from a function fitted to the IMFPs for each element was 0.89 Å and that the average of the mean percentage deviations *R* for each element of the individual IMFPs from the fitted IMFPs was 4.4 % [19]. The corresponding value of *RMS* and average value of *R* for the measured IMFPs were 3.00 Å and 13.2 %, respectively [19]; these values are about three times larger than the corresponding values for the calculated IMFPs. Finally, the value of *RMS* and average value of *R* for the measured IMFPs compared to the function fitted to the calculated IMFPs were 4.56 Å and 17.4 %, respectively [19]. In these various comparisons, it was found that the values of *RMS* and *R* for Ni, Cu, Ag, and Au were appreciably less than the corresponding average values for the group of seven elements. For these elements, “recommended IMFPs” were derived from a function fitted to the calculated IMFPs for each element [19].

The values of *RMS* and *R* in the above-mentioned comparisons should be considered as lower limits to the IMFP uncertainty because it has not been possible to quantify other potential sources of systematic error in the calculations and measurements [19]. In the absence of more detailed knowledge of the systematic errors in the IMFP calculations and measurements, the average value of *RMS* = 4.56 Å found in the comparison of measured IMFPs with the function fitted to the calculated IMFPs for each of the seven elements and the corresponding average value of *R* = 17.4 % will be considered as reasonable estimates of the IMFP standard uncertainty.

For some elements and compounds, the database contains more than one source of calculated or measured IMFPs. In general, it has not been possible to quantify the uncertainties in individual IMFP measurements or calculations. Until this can be done, no guidance can be given to a preferred source of data. The “recommended IMFPs” should nevertheless be used for Ni, Cu, Ag, and Au. For these four elements, calculated and measured IMFPs from other sources are also provided so that users can access these data if they wish to (or if future analyses show that IMFPs from particular sources have a lower uncertainty).

There is an additional source of uncertainty in IMFPs from the database arising from the use of analytical functions to fit the calculated and measured IMFPs from each source so that interpolations could be made. Information on this uncertainty is given elsewhere [19,20].

For materials for which there are no direct IMFP calculations or measurements, IMFPs can be obtained conveniently from two predictive formulae in the database, the TPP-2M equation of Tanuma *et al.* [21] and the G-1 equation of Gries [22]. These two equations are described in Appendix B.

Comparison of IMFPs from the TPP-2M equation with those directly calculated from optical data showed average RMS deviations of 10.2% for a group of 27 elements, 8.5 % for a group of 14 organic compounds, and 18.9% for a group of 15 inorganic compounds [21]. These deviations were considered to be satisfactorily small on account of the similar uncertainty of the optical data used in the IMFP calculations and the empirical nature of the TPP-2M equation. The larger deviations found for the inorganic compounds were expected because the optical data for these compounds had greater uncertainties than for the other materials. Comparisons of IMFPs calculated from the TPP-2M equation for Ni, Cu, Ag, and Au with the corresponding recommended IMFPs for these elements show satisfactory agreement [20]. The average value of *RMS* between IMFPs from the TPP-2M equation and the corresponding recommended IMFPs was 0.90 Å and the corresponding value of *R* was 10.9 % [20].

The uncertainties of IMFPs obtained from the TPP-2M equation can be expressed in two ways depending on the intended application of the data. If, for example, IMFPs for two materials are to be compared, then the standard uncertainty of each is estimated from the comparison with the recommended IMFPs to be 0.90 Å or 10.9 %. If absolute values of IMFPs are required, the standard uncertainty will be the quadrature sum of one of these values and the corresponding uncertainty found in the comparison of measured and calculated IMFPs (4.56 Å and 17.4% for *RMS* and *R*, respectively). This combined standard uncertainty is thus estimated to be 4.7 Å or 20.5 %.

There is one additional source of uncertainty in the use of the TPP-2M equation. For some elements, it is not clear whether the parameter  $N_v$  should be simply the number of valence electrons, as defined in Appendix B, or whether this number should be increased to include the number of core electrons with binding energies of less than about 30 eV [23]. For some elements (listed in Table B.1),  $N_v$  has been increased to include these shallow core electrons but for others the core electrons have been excluded. In some cases, the inclusion or exclusion of the shallow core electrons does not lead to changes of more than 20 % in the IMFPs calculated from the TPP-2M equation but larger changes can be found for other elements [23].

The G-1 predictive IMFP equation [22] was developed from an analysis of the calculated IMFPs of Tanuma *et al.* [21,24,25] over the 200 eV to 2000 eV range and an atomistic model of inelastic electron scattering. The G-1 equation has a different dependence on material parameters than the TPP-2M equation of Tanuma *et al.* At an energy of 2 keV, the average deviations between IMFPs from the G-1 equation and IMFPs of Tanuma *et al.* were similar in magnitude to those reported by Tanuma *et al.* [21] for their TPP-2M equation (although it should be noted that the comparisons of Tanuma *et al.* were made over the 50 eV to 2000 eV energy range).

Tanuma *et al.* [26] have analyzed the Gries model and have pointed out some important limitations. Although the G-1 equation provides useful estimates of IMFPs for many elements and compounds, there can be substantial deviations (of up to about 50%) for a few of the materials that have been examined to date. Since there is presently no explanation for these deviations, it is believed that the TPP-2M equation has greater general reliability [26]. Although use of the G-1 equation requires knowledge of just one material parameter (the specimen

density), it is recommended that IMFPs be determined from this equation only if a user has reason to believe that the TPP-2M equation will not give satisfactory results.

Further information on the uncertainties of IMFP data is given in two recent reviews [18,52].

### **Uncertainties of TMFP Data**

Values of TMFPs are obtained from differential elastic-scattering cross sections for free atoms [8,15,16,27]. For Be, C, Al, Cu, Ag, and Au at an energy of 1000 eV, the calculated TMFPs can vary between – 8.5 % and 4.0 % depending on whether the differential elastic-scattering cross sections were calculated from Thomas-Fermi-Dirac (TFD) or Dirac-Hartree-Fock-Slater (DHFS) potentials [15,27]. Similar comparisons between TMFPs from the TFD and Dirac-Hartree-Fock (DHF) potentials [15,28] showed differences between – 9.2 % and 3.8 % [27]. Comparisons were also made between TMFPs for the same elements from TFD and DHF potentials at selected energies between 100 eV and 10,000 eV. The largest deviation (30 %) was for Cu at 100 eV [27]. For the other five elements, the largest percentage deviations were between 10 % and 20 % at energies less than 250 eV; the percentage deviations became smaller with increasing energy above 250 eV [27,28]. Since the TMFP is typically larger than the IMFP for AES and XPS [6], the relative contribution of uncertainties in the TMFP data (derived from the TFD potential [8]) is generally less than the uncertainties of the IMFP data.

The TMFP describes the mean fractional momentum loss due to elastic-electron scattering alone, and is mainly determined by the differential cross section for large-angle elastic-scattering events [28]. While the interaction potential for elastic scattering in a solid is certainly different from the potential for an isolated atom, this difference leads mainly to changes in the differential cross section for small-angle scattering events. Cumpson and Seah [10] compared values of EALs obtained from Monte Carlo simulations made with two potentials, an atomic Hartree-Fock-Slater potential and a solid-state muffin-tin potential, for 18 elements at energies between 50 eV and 2000 eV. They found that the standard deviation of differences between EALs from the two potentials was about 2.5 % at 200 eV and 1.5 % at 1000 eV; these differences are small compared to other uncertainties.

### **Uncertainties of Transport Approximation**

Practical EALs calculated from this database with the overlayer-film definition and use of the transport approximation for Si 2s, Si 2p<sub>3/2</sub>, Au 4s, and Au 4f<sub>7/2</sub> photoelectrons excited by Mg K $\alpha$  x-rays have been compared with EALs obtained from Monte Carlo simulations [6]. The average of the percentage deviations between the EALs from the two approaches for various overlayer thicknesses and emission angles was 5.28 % [6]. Additional comparisons were made between average practical EALs from the database for the principal photoelectron and Auger-electron lines of Si, Cu, Ag, and W at an emission angle of 45° and similar EALs derived from Monte Carlo simulations by Cumpson and Seah [10]. A root-mean-square deviation of 1.6 % was found between the two approaches [6]. The uncertainty in EALs due to use of the transport approximation thus appeared to be appreciably less than the uncertainty of the IMFP data [6]. Powell *et al.* [29,30], however, have reported systematic differences between EALs derived from the transport approximation and values obtained from Monte Carlo simulations, particularly for

substrate/film combinations that have differences in elastic- and inelastic-scattering parameters for each material.

### **Uncertainties of DDF Data**

Monte Carlo simulations have been performed to determine the sensitivity of the DDF to the choice of interaction potential used in calculations of differential elastic-scattering cross sections [27]. These simulations were made for cross sections from the TFD and DHFS potentials and for XPS in a typical experimental configuration with Be 1s, C 1s, Al 2s, Cu 3s, Ag 4s, and Au 5s photoelectrons excited by Mg K $\alpha$  x-rays. Any significant difference between the DDFs from the two approaches was overshadowed by random statistical errors associated with the Monte Carlo simulations. Most percentage deviations were less than  $\pm 10\%$  [27].

Comparisons have also been made between DDFs calculated from the transport approximation (with TMFPs obtained from differential elastic-scattering cross sections computed with the TFD potential [8]) and DDFs from Monte Carlo simulations [28]. These comparisons involved 360 simulations (XPS with different solids, different asymmetry parameters, and different photoelectron energies) for emission angles between  $0^\circ$  and  $70^\circ$ . In most cases, the percentage differences between DDFs from the two approaches were less than 10%, while the largest value was 11.7% [31].

### **Uncertainties of CF Data**

The uncertainties of the CF data are the same as the uncertainties of the DDF data.

## VI. REFERENCES

1. Jablonski, A., and Powell, C. J., *Surf. Science Reports* 47, 33 (2002).
2. Tilinin, I. S., Jablonski, A., Zemek, J., and Hucek, S., *J. Electron Spectrosc. Relat. Phenom.* 87, 127 (1997).
3. Powell, C. J., and Jablonski, A., *J. Electron Spectrosc. Relat. Phenom.* 114-116, 1139 (2001).
4. Powell, C. J., and Jablonski, A., *Surf. Science* 488, L547 (2001).
5. Jablonski, A., and Powell, C. J., *J. Vac. Sci. Tech. A* 27, 253 (2009).
6. Powell, C. J., and Jablonski, A., *Surf. Interface Anal.* 33, 211 (2002).
7. Powell, C. J., and Jablonski, A., *NIST Electron Inelastic-Mean-Free-Path Database (SRD 71)*, Version 1.1, National Institute of Standards and Technology, Gaithersburg, MD (2001).
8. Jablonski, A., *NIST Electron Elastic-Scattering Cross-Section Database (SRD 64)*, Version 2.0, National Institute of Standards and Technology, Gaithersburg, MD (2000).
9. Jablonski, A., *Phys. Rev. B* 58, 16470 (1998).
10. Cumpson, P. J., and Seah, M. P., *Surf. Interface Anal.* 25, 430 (1997).
11. Jablonski, A., and Powell, C. J., *J. Electron Spectrosc. Relat. Phenom.* 100, 137 (1999); *ibid.* 107, 201 (2000).
12. Jablonski, A., *Surf. Science* 364, 380 (1996).
13. Jablonski, A., and Tilinin, I. S., *J. Electron Spectrosc. Relat. Phenom.* 74, 207 (1995).
14. Jablonski, A., and Tougaard, S., *Surf. Interface Anal.* 26, 374 (1998).
15. Jablonski, A., Salvat, F., and Powell, C. J., *J. Phys. Chem. Ref. Data* 33, 409 (2004).
16. Jablonski, A., Salvat, F., and Powell, C. J., *NIST Electron Elastic-Scattering Cross-Section Database (SRD 64)*, Version 3.1, National Institute of Standards and Technology, Gaithersburg, MD (2003).
17. Jablonski, A., and Powell, C. J., *Surf. Science* 520, 78 (2002).
18. Powell, C. J., and Jablonski, A., *Nucl. Instr. Meth. Phys. Res. A* 601, 54 (2009).
19. Powell, C. J., and Jablonski, A., *J. Phys. Chem. Ref. Data* 28, 19 (1999).
20. Powell, C. J., and Jablonski, A., *Surf. Interface Anal.* 29, 108 (2000).
21. Tanuma, S., Powell, C. J., and Penn, D. R., *Surf. Interface Anal.* 21, 165 (1994).
22. Gries, W. H., *Surf. Interface Anal.* 24, 38 (1996).
23. Tanuma, S., Powell, C. J., and Penn, D. R., *Surf. Interface Anal.* 35, 268 (2003).
24. Tanuma, S., Powell, C. J., and Penn, D. R., *Surf. Interface Anal.* 17, 911 (1991).
25. Tanuma, S., Powell, C. J., and Penn, D. R., *Surf. Interface Anal.* 17, 927 (1991).
26. Tanuma, S., Powell, C. J., and Penn, D. R., *Surf. Interface Anal.* 25, 25 (1997).
27. Jablonski, A., and Powell, C. J., *Surf. Science* 463, 29 (2000).
28. Mayol, R., and Salvat, F., *Atom. Data Nucl. Data Tables* 65, 55 (1997).
29. Powell, C. J., Jablonski, A., Werner, W. S. M., Smekal, W., *Appl. Surf. Science* 239, 470 (2005); *erratum* 242, 219 (2005).
30. Powell, C. J., Werner, W. S. M., and Smekal, W., *Appl. Phys. Letters* 89, 252116 (2006).
31. Jablonski, A., and Tougaard, S., *Surf. Science* 432, 211 (1999).
32. Powell, C. J., *Appl. Surf. Science* 89, 141 (1995).
33. *NIST X-ray Photoelectron Spectroscopy Database*, SRD 20, Version 3.5, National Institute of Standards and Technology, Gaithersburg, MD (2008).
34. Moulder, J. F., Stickle, W. F., Sobol, P. E., and Bomben, K. D., *Handbook of X-ray Photoelectron Spectroscopy* (Perkin-Elmer Corporation, Physical Electronics Division, Eden Prairie, 1992).

35. Band, I. M., Kharitonov, Yu. I., and Trzhaskovskaya, M. B., *At. Data Nucl. Data Tables* 23, 443 (1979).
36. Schweppe, J., Deslattes, R. D., Mooney, T., and Powell, C. J., *J. Electron Spectrosc. Relat. Phenom.* 67, 463 (1994).
37. Tanuma, S., Powell, C. J., and Penn, D. R., *Surf. Interface Anal.* 11, 577 (1988).
38. Seah, M. P., and Gilmore, I. S., *Surf. Interface Anal.* 26, 908 (1998).
39. Seah, M. P., Gilmore, I. S., and Spencer, S. J., *J. Vac. Sci. Technol. A* 18, 1083 (2000).
40. Smith, D. M., Gallon, T. E., and Matthew, J. A. D., *J. Phys. B* 7, 1255 (1974).
41. Netzer, F. P., and Matthew, J. A. D., *Rep. Prog. Phys.* 49, 621 (1986).
42. *American Institute of Physics Handbook*, D. E. Gray, ed. (McGraw-Hill, New York, 1963), p. 9-22.
43. Ashcroft, N. W., and Mermin, N. D., *Solid State Physics* (Holt, Rinehart and Winston, 1976), p. 566.
44. Kittel, C., *Introduction to Solid State Physics*, sixth edition (John Wiley, New York, 1986), p. 185.
45. Wolfe, C. M., Holonyak, J., and Stillman, G. E., *Physical Properties of Semiconductors* (Prentice-Hall, Englewood Cliffs, 1989).
46. *CRC Handbook of Chemistry and Physics*, 77th edition, D. R. Lide, ed. (CRC Press, Boca Raton, 1996), pp. 12-94–12-98.
47. W. H. Strehlow and E. L. Cook, *J. Phys. Chem. Ref. Data* 2, 163 (1973).
48. Tanuma, S., Powell, C. J., and Penn, D. R., *Surf. Interface Anal.* 20, 77 (1993).
49. Coplen, T. B., *Pure Appl. Chem.* 68, 2339 (1996).
50. *CRC Handbook of Chemistry and Physics*, 77th edition, D. R. Lide, ed. (CRC Press, Boca Raton, 1996), pp 4-37–4-98.
51. *CRC Handbook of Chemistry and Physics*, 77th edition, D. R. Lide, ed. (CRC Press, Boca Raton, 1996), pp 3-3–3-330.
52. Powell, C. J., and Jablonski, A., *J. Electron Spectrosc. Relat. Phenom.* 178-179, 331 (2010).
53. Seah, M. P., and Gilmore, I. S., *Surf. Interface Anal.* 31, 835 (2001).

## APPENDIX A

### VALUES OF ELECTRON BINDING ENERGIES AND OF THE PHOTOIONIZATION ASYMMETRY PARAMETER $\beta$

Table A.1 contains values of elemental core-electron binding energies (BEs) and of the photoionization asymmetry parameter  $\beta$  for use in EAL calculations for XPS with Mg and Al  $K\alpha$  x-rays. Many of the BEs were taken from the analysis of Powell [32] and the majority of the remaining entries are average values from the NIST XPS Database [33]. For elements that are normally gaseous, the listed BE is the average of the minimum and maximum BEs for compounds in the NIST XPS Database [33]. Other BEs were obtained from the Physical Electronics *Handbook of X-ray Photoelectron Spectroscopy* [34]. Values of  $\beta$  were calculated by Band *et al.* [35].

The kinetic energy of photoelectrons is given by the difference between the particular x-ray energy (1253.6 eV for Mg  $K\alpha$  x-rays and 1486.6 eV for Al  $K\alpha$  x-rays [36]) and the relevant core-electron binding energy. Small changes in binding energies for an element in different chemical states should normally have a negligible effect on the EAL (although IMFPs may change with chemical state).

**Table A.1.** Values of elemental electron binding energies [32-34] and of the photoionization asymmetry parameter  $\beta$  [35] for XPS with Mg and Al  $K\alpha$  x-rays for the indicated elements and subshells.

Element	Subshell	Binding Energy (eV)	$\beta$	
			Mg x-rays	Al x-rays
Li	1s	55.0	2.00	2.00
Be	1s	111.9	2.00	2.00
B	1s	188.6	2.00	2.00
C	1s	284.4	2.00	2.00
N	1s	401.7	2.00	2.00
O	1s	533.4	2.00	2.00
F	1s	688.5	2.00	2.00
Ne	1s	862.5	2.00	2.00
Na	1s	1071.4	2.00	2.00
	2s	63.6	2.00	2.00
	2p <sub>3/2</sub>	30.6	0.87	0.79
Mg	1s	1303.3	2.00	
	2s	63.6	2.00	2.00
	2p <sub>3/2</sub>	49.8	0.96	0.88
Al	2s	118.1	2.00	2.00
	2p <sub>3/2</sub>	72.9	1.04	0.96

Si	2s	150.7	2.00	2.00
	2p <sub>3/2</sub>	99.3	1.11	1.03
P	2s	187.9	2.00	2.00
	2p <sub>3/2</sub>	130.0	1.18	1.10
S	2s	229.2	2.00	2.00
	2p <sub>3/2</sub>	163.8	1.23	1.16
Cl	2s	270.3	2.00	2.00
	2p <sub>3/2</sub>	202.5	1.29	1.22
Ar	2p <sub>3/2</sub>	241.8	1.33	1.27
K	2s	379.2	2.00	2.00
	2p <sub>3/2</sub>	294.7	1.37	1.31
	3p <sub>3/2</sub>	18.7	1.32	1.26
Ca	2s	440	2.00	2.00
	2p <sub>3/2</sub>	346.6	1.40	1.35
	3p <sub>3/2</sub>	25.6	1.36	1.30
Sc	2p <sub>3/2</sub>	398.5	1.43	1.38
	3p <sub>3/2</sub>	29.2	1.40	1.34
Ti	2p <sub>3/2</sub>	454.0	1.45	1.41
	3p <sub>3/2</sub>	32.5	1.43	1.37
V	2p <sub>3/2</sub>	512.2	1.46	1.43
	3p <sub>3/2</sub>	37.2	1.46	1.40
Cr	2p <sub>3/2</sub>	574.4	1.47	1.45
	3p <sub>3/2</sub>	42.3	1.48	1.43
Mn	2p <sub>3/2</sub>	638.9	1.47	1.46
	3p <sub>3/2</sub>	47.2	1.50	1.46
Fe	2p <sub>3/2</sub>	706.9	1.46	1.47
	3p <sub>3/2</sub>	52.5	1.52	1.48
Co	2p <sub>3/2</sub>	778.4	1.44	1.47
	3p <sub>3/2</sub>	58.9	1.54	1.50
Ni	2p <sub>3/2</sub>	852.7	1.41	1.46
	3p <sub>3/2</sub>	66.1	1.56	1.52
Cu	2p <sub>3/2</sub>	932.7	1.34	1.44
	3p <sub>3/2</sub>	75.1	1.57	1.54
Zn	2p <sub>3/2</sub>	1021.8	1.25	1.41
	3p <sub>3/2</sub>	88.6	1.58	1.55
	3d <sub>5/2</sub>	10.0	1.05	0.99
Ga	2p <sub>3/2</sub>	1117.1	1.08	1.36
	3p <sub>3/2</sub>	104.5	1.60	1.57
	3d <sub>5/2</sub>	18.6	1.07	1.02
Ge	2p <sub>3/2</sub>	1217.3	0.67	1.27
	3p <sub>3/2</sub>	121.5	1.60	1.58
	3d <sub>5/2</sub>	29.4	1.09	1.04
As	2p <sub>3/2</sub>	1323.5	1.12	
	3p <sub>3/2</sub>	140.8	1.61	1.59
	3d <sub>5/2</sub>	41.7	1.11	1.06



Se	3p <sub>3/2</sub>	161.5	1.62	1.60
	3d <sub>5/2</sub>	55.1	1.13	1.08
Br	3p <sub>3/2</sub>	184.8	1.62	1.61
	3d <sub>5/2</sub>	68.9	1.15	1.10
Kr	3p <sub>3/2</sub>	207.5	1.63	1.62
	3d <sub>5/2</sub>	87.0	1.16	1.12
Rb	3p <sub>3/2</sub>	239.1	1.63	1.62
	3d <sub>5/2</sub>	112	1.18	1.14
Sr	3p <sub>3/2</sub>	268.4	1.63	1.63
	3d <sub>5/2</sub>	134.3	1.19	1.15
Y	3p <sub>3/2</sub>	299.3	1.63	1.63
	3d <sub>5/2</sub>	155.8	1.20	1.17
Zr	3p <sub>3/2</sub>	329.8	1.63	1.63
	3d <sub>5/2</sub>	178.8	1.21	1.18
Nb	3p <sub>3/2</sub>	360.6	1.63	1.64
	3d <sub>5/2</sub>	202.3	1.21	1.19
Mo	3p <sub>3/2</sub>	394.8	1.62	1.63
	3d <sub>5/2</sub>	228.0	1.22	1.20
Ru	3p <sub>3/2</sub>	461.5	1.60	1.63
	3d <sub>5/2</sub>	280.1	1.22	1.21
Rh	3p <sub>3/2</sub>	496.5	1.59	1.62
	3d <sub>5/2</sub>	307.2	1.22	1.22
Pd	3p <sub>3/2</sub>	532.3	1.57	1.62
	3d <sub>5/2</sub>	335.1	1.22	1.22
Ag	3p <sub>3/2</sub>	573.1	1.56	1.61
	3d <sub>5/2</sub>	368.3	1.21	1.22
Cd	3p <sub>3/2</sub>	618.4	1.53	1.60
	3d <sub>5/2</sub>	405.1	1.20	1.22
In	3p <sub>3/2</sub>	665.6	1.51	1.58
	3d <sub>5/2</sub>	443.9	1.19	1.22
	4d <sub>5/2</sub>	16.7	1.31	1.29
Sn	3p <sub>3/2</sub>	714.7	1.48	1.56
	3d <sub>5/2</sub>	485.0	1.18	1.21
	4d <sub>5/2</sub>	23.9	1.32	1.30
Sb	3p <sub>3/2</sub>	766.4	1.44	1.54
	3d <sub>5/2</sub>	528.3	1.16	1.21
	4d <sub>5/2</sub>	32.0	1.33	1.31
Te	3p <sub>3/2</sub>	819.6	1.39	1.52
	3d <sub>5/2</sub>	573.0	1.14	1.20
	4d <sub>5/2</sub>	40.4	1.33	1.32
I	3p <sub>3/2</sub>	875	1.33	1.49
	3d <sub>5/2</sub>	622.9	1.11	1.18
	4d <sub>5/2</sub>	49.7	1.33	1.32
Xe	3d <sub>5/2</sub>	669.6	1.08	1.17
	4d <sub>5/2</sub>	60.8	1.34	1.33

Cs	3d <sub>5/2</sub>	726.2	1.04	1.15
	4d <sub>5/2</sub>	77.4	1.34	1.33
Ba	3d <sub>5/2</sub>	780.1	1.00	1.12
	4d <sub>5/2</sub>	90.2	1.34	1.34
La	3d <sub>5/2</sub>	835.9	0.95	1.10
	4d <sub>5/2</sub>	103.9	1.34	1.34
Ce	3d <sub>5/2</sub>	883.7	0.88	1.06
	4d <sub>5/2</sub>	111.2	1.34	1.34
Pr	3d <sub>5/2</sub>	931.9	0.82	1.02
	4d <sub>5/2</sub>	115	1.34	1.34
Nd	3d <sub>5/2</sub>	980.9	0.73	0.98
	4d <sub>5/2</sub>	121	1.33	1.34
Sm	3d <sub>5/2</sub>	1081.2	0.53	0.86
	4d <sub>5/2</sub>	129	1.33	1.34
Eu	3d <sub>5/2</sub>	1126	0.44	0.80
	4d <sub>5/2</sub>	128.2	1.32	1.34
Gd	3d <sub>5/2</sub>	1186	0.42	0.72
	4d <sub>5/2</sub>	140.4	1.32	1.34
Tb	3d <sub>5/2</sub>	1239.4		0.62
	4d <sub>5/2</sub>	146.0	1.31	1.34
Dy	3d <sub>5/2</sub>	1296		0.53
	4d <sub>5/2</sub>	152.4	1.30	1.33
Ho	4d <sub>5/2</sub>	159.6	1.29	1.33
Er	4d <sub>5/2</sub>	167.3	1.28	1.32
Tm	4d <sub>5/2</sub>	175.4	1.27	1.32
Yb	4d <sub>5/2</sub>	182.4	1.26	1.31
Lu	4d <sub>5/2</sub>	196.3	1.25	1.30
Hf	4d <sub>5/2</sub>	211.5	1.24	1.29
	4f <sub>7/2</sub>	14.3	1.05	1.06
Ta	4d <sub>5/2</sub>	226.4	1.22	1.29
	4f <sub>7/2</sub>	21.8	1.04	1.06
W	4d <sub>5/2</sub>	243.5	1.21	1.28
	4f <sub>7/2</sub>	31.4	1.04	1.05
Re	4d <sub>5/2</sub>	260.5	1.20	1.27
	4d <sub>7/2</sub>	40.3	1.04	1.05
Os	4d <sub>5/2</sub>	278.5	1.18	1.26
	4f <sub>7/2</sub>	50.7	1.03	1.05
Ir	4d <sub>5/2</sub>	296.3	1.17	1.25
	4f <sub>7/2</sub>	60.8	1.03	1.05
Pt	4d <sub>5/2</sub>	314.6	1.14	1.23
	4f <sub>7/2</sub>	71.1	1.02	1.04
Au	4d <sub>5/2</sub>	335.2	1.12	1.22
	4f <sub>7/2</sub>	84.0	1.01	1.04
Hg	4d <sub>5/2</sub>	359.3	1.10	1.20
	4f <sub>7/2</sub>	99.9	1.01	1.04
Tl	4d <sub>5/2</sub>	385.0	1.08	1.19

	4f <sub>7/2</sub>	117.7	1.00	1.03
Pb	4d <sub>5/2</sub>	412.0	1.05	1.17
	4f <sub>7/2</sub>	136.9	0.99	1.03
Bi	4d <sub>5/2</sub>	440.1	1.02	1.15
	4f <sub>7/2</sub>	157.0	0.98	1.02
Th	4d <sub>5/2</sub>	675.2	0.77	0.98
	4f <sub>7/2</sub>	333.3	0.89	0.97
U	4d <sub>5/2</sub>	736.5	0.67	0.91
	4f <sub>7/2</sub>	377.1	0.86	0.94

---

## APPENDIX B

### PREDICTIVE FORMULAE FOR ELECTRON INELASTIC MEAN FREE PATHS

IMFPs can be obtained conveniently from two predictive formulae, the TPP-2M equation of Tanuma *et al.* [21] and the G-1 equation of Gries [22]. These formulae will now be described in turn. Information on atomic weights and elemental densities is given in the final section.

#### TPP-2M Equation of Tanuma, Powell, and Penn

Tanuma *et al.* [21] proposed the following equations for the calculation of the IMFP  $\lambda$  (in Ångstroms) as a function of electron energy  $E$  (in eV) and various material parameters:

$$\lambda = \frac{E}{E_p^2 [\beta \ln(\gamma E) - (C/E) + (D/E^2)]} \quad (\text{B.1})$$

where

$$\beta = -0.10 + 0.944/(E_p^2 + E_g^2)^{1/2} + 0.069\rho^{0.1} \quad (\text{B.2})$$

$$\gamma = 0.191\rho^{-0.50} \quad (\text{B.3})$$

$$C = 1.97 - 0.91U \quad (\text{B.4})$$

$$D = 53.4 - 20.8U \quad (\text{B.5})$$

$$U = N_v\rho/M = E_p^2/829.4 \quad (\text{B.6})$$

and  $E_p = 28.8 (N_v\rho/M)^{1/2}$  is the free-electron plasmon energy (in eV),  $\rho$  is the density (in  $\text{g cm}^{-3}$ ),  $N_v$  is the number of valence electrons per atom (for an element) or molecule (for a compound),  $M$  is the atomic or molecular weight, and  $E_g$  is the bandgap energy (in eV). Equations (B.1) through (B.6) are collectively known as the TPP-2M equation.

Table B.1 shows recommended elemental values for the parameter  $N_v$  in the TPP-2M equation. During the development of the TPP-2M equation, there was ambiguity in the choice of a value of  $N_v$  for elements in which there were core-levels with binding energies less than about 30 eV [23,37]. Recent measurements of Auger-electron yields for many solid elements by Seah and Gilmore [38], however, have given experimental guidance on the appropriate choice of  $N_v$  for many elements. For the rare-earth elements, these authors recommended that the 4f electrons should be excluded in the count for  $N_v$ . In more recent work from the same group, however, the recommended choices for the rare-earth elements have been revised to include the 4f electrons [39]. Comparisons of IMFPs calculated from optical data for Gd, Tb, and Dy with IMFPs obtained from the TPP-2M equation and various values of  $N_v$  nevertheless indicate that the 4f electrons should be excluded [23]. This conclusion is supported by an analysis of the energy-loss

function for these three elements [23] and the expectation that the 4f electrons do not contribute substantially to the energy-loss function for energy losses less than about 50 eV [40]. On this basis, values of  $N_v$  for the rare earths in Table A.1 have been computed from the sum of the chemical valence [41] and the 6 5p electrons that contribute strongly to the energy-loss spectrum [23]. There is now a non-physical discontinuity, however, between the  $N_v$  values for the rare earths and those for Cs, Ba, and La. Further work is needed to establish the influence of 5p-electron excitations in the latter three elements and of similar core-electron excitations for other elements in groups IA, II, and III of the Periodic Table [23].

For compounds,  $N_v$  is calculated from the sum of contributions from each constituent element (i.e.,  $N_v$  for each element multiplied by the chemical or estimated stoichiometric coefficient for that element).

Values of the bandgap energy  $E_g$  for many compounds can be found in a number of sources [42-47]. Table B.2 contains values of  $E_g$  for some elements and representative compounds. If a value for the bandgap energy  $E_g$  cannot be found for the compound of interest, it is satisfactory to estimate this parameter because the IMFP is not a sensitive function of  $E_g$  [25,48]. For highly ionic compounds such as the alkali halides,  $E_g$  is generally between 6 eV and 11 eV. For oxides,  $E_g$  are often between 1 eV and 9 eV.

**Table B.1.** Recommended values for the number of valence electrons per atom (the parameter  $N_v$ ) for each element for calculation of IMFPs from the TPP-2M predictive IMFP equation [21,23].

Z	Element	$N_v$
1	H	1
2	He	2
3	Li	1
4	Be	2
5	B	3
6	C	4
7	N	5
8	O	6
9	F	7
10	Ne	8
11	Na	1
12	Mg	2
13	Al	3
14	Si	4
15	P	5
16	S	6
17	Cl	7
18	Ar	8
19	K	1

20	Ca	2
21	Sc	3
22	Ti	4
23	V	5
24	Cr	6
25	Mn	7
26	Fe	8
27	Co	9
28	Ni	10
29	Cu	11
30	Zn	12
31	Ga	3
32	Ge	4
33	As	5
34	Se	6
35	Br	7
36	Kr	8
37	Rb	1
38	Sr	2
39	Y	3
40	Zr	4
41	Nb	5
42	Mo	6
44	Ru	8
45	Rh	9
46	Pd	10
47	Ag	11
48	Cd	12
49	In	3
50	Sn	4
51	Sb	5
52	Te	6
53	I	7
54	Xe	8
55	Cs	1
56	Ba	2
57	La	3
58	Ce	9
59	Pr	9
60	Nd	9
62	Sm	9
63	Eu	8
64	Gd	9
65	Tb	9
66	Dy	9
67	Ho	9

68	Er	9
69	Tm	9
70	Yb	8
71	Lu	9
72	Hf	4
73	Ta	5
74	W	6
75	Re	7
76	Os	8
77	Ir	9
78	Pt	10
79	Au	11
80	Hg	12
81	Tl	3
82	Pb	4
83	Bi	5
90	Th	4
91	Pa	3
92	U	3

**Table B.2.** Values of the band gap energy  $E_g$  for elements and selected compounds (at room temperature) from the indicated references for calculation of IMFPs from the TPP-2M predictive IMFP equation [21].

Material	$E_g$ (eV)	Reference
B	1.55	44
C (diamond)	5.4	44
Ge	0.67	44
Se (gray)	1.5	44
Si	1.107	44
Sn (alpha phase)	0.08	44
Te	0.33	44
AgBr	2.50	44
AgCl	3.0	40
AgI	2.63	44
AlAs	2.16	44
AlN	6.02	44
AlP	2.5	40
AlSb	1.60	44
BN	4.6	44
CdS	2.42	44
CdSe	1.74	44

CdTe	1.5	44
Cu <sub>2</sub> O	2.2	40
GaAs	1.35	44
GaN	3.34	44
GaP	2.24	44
GaSb	0.67	44
HgTe	0.2	40
InAs	0.36	44
InN	2.0	44
InP	1.27	44
InSb	0.16	44
KCl	8.5	40
MgO	7.3	40
NaCl	8.6	40
PbS	0.5	44
PbSe	0.37	44
PbTe	0.25	44
SiC (alpha phase)	2.86	44
TiO <sub>2</sub> (rutile)	3.05	40
ZnO	3.2	44
ZnS	3.6	44
ZnSb	0.56	44
ZnSe	2.58	44
ZnTe	2.26	44

---

### G-1 Equation of Gries

Gries [22] developed the following equation for the prediction of the IMFP  $\lambda$  (in Ångstroms):

$$\lambda = 10k_1(V_a / Z^*)E/(\log E - k_2) \quad (\text{B.7})$$

where  $V_a = M/\rho$  is the atomic volume (in  $\text{cm}^3 \text{mol}^{-1}$ ),  $Z^*$  is a parameter found empirically to be equal to  $Z^{1/2}$ ,  $Z$  is the atomic number (for an element), and  $k_1$  and  $k_2$  are parameters. Values of  $k_1$  and  $k_2$  were found from fits of Eq. (B.7) to the IMFPs calculated by Tanuma *et al.* [21,24,25] for groups of selected elements and compounds: 0.0020 and 1.30 for the 3d elements (Ti-Cu); 0.0019 and 1.35 for the 4d elements (Zr-Ag); 0.0019 and 1.45 for the 5d elements (Hf-Au); 0.0014 and 1.10 for the remaining elements (with which Y is included instead of the 4d elements; 0.0018 and 1.00 for organic compounds; and 0.0019 and 1.30 for inorganic compounds. The terms  $V_a$  and  $Z^*$  in Eq. (B.7) were generalized by Gries to apply to a compound  $A_pB_q, \dots C_r$ , with corresponding atomic numbers  $Z_A, Z_B, \dots Z_C$  and atomic weights  $M_A, M_B, \dots M_C$ , as follows:

$$Z^* = (pZ_A^{1/2} + qZ_B^{1/2} + \dots + Z_C^{1/2})/(p + q + \dots + r) \quad (\text{B.8})$$



$$V_a = (pM_A + qM_B + \dots + rM_C) / \rho(p + q + \dots + r) \quad (\text{B.9})$$

Equations (B.7) through (B.9) constitute the G-1 equation.

### Atomic Weight and Density Data

Numerical data for atomic weights and material densities are needed for evaluation of the TPP-2M equation of Tanuma *et al.* and the G-1 equation of Gries.

The database makes use of atomic weights recommended by the International Union of Pure and Applied Chemistry in 1995 [49]. Elemental densities have been obtained from Ref. 50. Other Handbooks containing density data were reviewed and numerous (generally small) discrepancies were found. Since the conditions of measurement in the various sources were not specified (and no references were provided), it was not possible to make a selection of data on scientific criteria. Instead, densities from Ref. 50 have been arbitrarily assumed to be "correct." If more reliable density data becomes available for particular elements, suitable adjustments can be made to IMFPs or EALs obtained from the database using the equations given above. The calculated IMFPs of Tanuma *et al.* for carbon in the database are for glassy carbon with a density of 1.8 g cm<sup>-3</sup> [24]; EALs can be calculated in the database with the Gries G-1 equation [Eqs. (B.7-B.9)] using either the density of graphite or of diamond. Densities for inorganic compounds and organic compounds can be obtained from Refs. 50 and 51, respectively.

Tanuma *et al.* developed an earlier predictive IMFP formula, designated TPP-2, based on calculated IMFPs for a group of 27 elements [24]; this predictive equation was later modified, in one parameter, to become the TPP-2M equation given above after consideration of calculated IMFPs for a group of 14 organic compounds [21]. The extent to which an IMFP calculated from the TPP-2 equation depends on material density has been analyzed for several representative elements and inorganic compounds [24,48]. Similar tests have not been made for the TPP-2M equation although it is thought that the earlier tests with the TPP-2 equation should provide general guidance. The database can, of course, be utilized to examine the variation of calculated EALs for a material of interest with different assumed densities in the TPP-2M and G-1 equations.

## APPENDIX C

### DEFINITIONS OF ELECTRON EFFECTIVE ATTENUATION LENGTHS

As discussed elsewhere [1,6,18,52], it is possible to define electron EALs for the measurement of overlayer-film thicknesses (the most common application) and of marker-layer depths. In addition, it is possible to define “local” EALs, useful for a small range of thicknesses or depths, and “practical” EALs, useful for thicknesses or depths likely to be of practical importance. Numerical differences between EALs from the different definitions for different materials and different experimental configurations are presented and discussed elsewhere [1,3-6].

The definitions of these different EALs are given below [1]. We also include definitions of the average practical EAL for a range of overlayer-film thicknesses [1] and of the effective attenuation length for quantitative analysis [1,6,18,52].

#### Local EALs

The local EAL,  $EAL$ , for the measurement of marker-layer depths is:

$$EAL = - \left[ \cos \alpha \frac{d \ln \phi(z, \alpha)}{dz} \right]^{-1} \quad (C.1)$$

where  $\phi(z, \alpha)$  is the emission depth distribution function for the signal electrons, a function of depth  $z$  and electron emission angle  $\alpha$  with respect to the surface normal.

The local EAL for the measurement of overlayer-film thicknesses is:

$$EAL = - \left[ \cos \alpha \frac{d}{dt} \ln \left( \int_t^\infty \phi(z, \alpha) dz \right) \right]^{-1} \quad (C.2)$$

where  $t$  is the thickness of the overlayer film.

#### Practical EALs

The practical EAL,  $L$ , for measurement of overlayer-film thicknesses is:

$$L = \frac{1}{\cos \alpha} \frac{t}{(\ln I_s^0 - \ln I_s)} = \frac{1}{\cos \alpha} \frac{t}{\left[ \ln \int_0^\infty \phi(z, \alpha) dz - \ln \int_t^\infty \phi(z, \alpha) dz \right]} \quad (C.3)$$

where  $I_s^0$  is the substrate-signal intensity from an uncovered substrate and  $I_s$  is the substrate-signal intensity after deposition of an overlayer film of thickness  $t$ .

The practical EAL for measurement of the depth  $z$  of a thin marker layer is:

$$L = \frac{1}{\cos \alpha} \frac{z}{\ln \phi(0, \alpha) - \ln \phi(z, \alpha)} \quad (\text{C.4})$$

### Average Practical EAL

The average practical EAL,  $L_{ave}$ , for various overlayer-film thicknesses  $t_i$  within a selected film-thickness range (from zero to a selected maximum thickness) is:

$$L_{ave} = \frac{1}{n} \sum_{i=1}^n \frac{1}{\cos \alpha} \frac{t_i}{[\ln \int_0^{\infty} \phi(z, \alpha) dz - \ln \int_{t_i}^{\infty} \phi(z, \alpha) dz]} \quad (\text{C.5})$$

where the thicknesses  $t_i$  are evenly distributed over the relevant range and  $n$  denotes the total number of considered thicknesses.

### EAL for Quantitative Analysis

The EAL for quantitative analysis,  $L_{QA}$ , is an EAL that replaces the IMFP in formulae derived for quantitative AES and XPS analyses on the assumption that elastic-scattering effects were negligible; this replacement provides a simple correction for elastic-scattering effects [1,6,52].

## APPENDIX D

### CUMPSON AND SEAH PREDICTIVE FORMULA FOR ELECTRON EFFECTIVE ATTENUATION LENGTHS

Cumpson and Seah [10] developed the following equation for the prediction of the average effective attenuation length for electrons of energy  $E$  in an elemental solid with atomic number  $Z$ :

$$EAL = 0.316a^{3/2} \left\{ \frac{E}{Z^{0.45} [\ln(E/27) + 3]} + 4 \right\} \text{ nanometers,} \quad (\text{D.1})$$

where  $a$  is the average lattice parameter in nanometers,

$$a = 10^8 \left( \frac{A_w}{\rho N_{Av}} \right)^{1/3}, \quad (\text{D.2})$$

and  $A_w$  is the average atomic weight (in g),  $\rho$  is the density (in kg/m<sup>3</sup>), and  $N_{Av}$  is the Avogadro constant ( $6.02 \times 10^{23} \text{ mol}^{-1}$ ). Equations (D.1) and (D.2) were designated the CS2 equation [10].

The CS2 equation was derived from EALs obtained from a different defining equation from those used in the database. The average EALs from the CS2 equation are applicable to a practically useful range of overlayer-film thicknesses in AES and XPS and for electron emission angles between 0° and 63° [10].

Average EALs reported by Cumpson and Seah for an emission angle of 45° agree closely with the average practical EALs from the database for some representative photoelectron and Auger-electron lines at an emission angle of 45° and for a range of overlayer-film thicknesses from zero to a value corresponding to attenuation of the substrate-signal intensity to 10 % of its original value (for an uncovered substrate) [3,5,6]. Poorer agreement is found with EALs from the CS2 equation [3,5,6].

## APPENDIX E

### OTHER PREDICTIVE FORMULAE FOR ELECTRON EFFECTIVE ATTENUATION LENGTHS

Seah and Gilmore [53] derived an analytical formula to represent the ratio of EALs obtained from the Monte Carlo simulations of Cumpson and Seah [10] for  $\alpha = 45^\circ$  to the corresponding IMFPs [24]:

$$L_{SG} / \lambda_i = 0.979[1 - \omega(0.955 - 0.0777 \ln Z)], \quad (\text{E.1})$$

where

$$\omega = \lambda_i / (\lambda_i + \lambda_t) \quad (\text{E.2})$$

is the single-scattering albedo, a convenient measure of the strength of elastic scattering,  $\lambda_i$  is the inelastic mean free path (IMFP) and  $\lambda_t$  is the transport mean free path (TMFP), a parameter derived from the transport cross section [15]. This formula for the EAL,  $L_{SG}$ , was recommended for emission angles in the range  $0^\circ \leq \alpha \leq 58^\circ$ . EALs from Eq. (E.1) agree better with EAL values from this database (obtained from the transport approximation) for Si, Cu, Ag, and W than the corresponding EALs from the Cumpson and Seah equation (Appendix D) [29].

Jablonski and Powell have reported an analytical formula similar to Eq. (E.1) [5]. Calculations were made, again using the algorithm based on solution of the kinetic Boltzmann equation within the transport approximation [2], of the ratio of the average EAL,  $L_{ave}$ , to the corresponding values of  $\lambda_i$  for selected photoelectron and Auger-electron lines of a group of elemental solids and inorganic compounds [5]. In these calculations,  $L_{ave}$  was determined for  $\psi = 54^\circ$  as the average value of the EAL for emission angles between  $0^\circ$  and  $50^\circ$  and for film thicknesses corresponding to attenuation of the substrate intensity to 1 %, 5 %, and 10 % of its maximum value. Plots of values of  $R_{EAL} = L_{ave} / \lambda_i$  as a function of  $\omega$  showed a simple linear dependence [5],

$$R_{EAL} = L_{ave} / \lambda_i = 1.0 - 0.735\omega. \quad (\text{E.3})$$

The average deviation of  $R_{EAL}$  values from the line was 0.61 %.

Values of  $\omega$  can be readily calculated using Eq. (E.2) with values of the IMFP and TMFP obtained from this database.

## APPENDIX F

### CONTACTS

If you have comments or questions about the database, the Standard Reference Data Program would like to hear from you. Also, if you have any problems with the CD-ROM or installation, please let us know by contacting:

Joan C. Sauerwein  
National Institute of Standards and Technology  
Standard Reference Data Program  
100 Bureau Drive, Stop 2310  
Gaithersburg, MD 20899-2310  
Internet: [srdata@nist.gov](mailto:srdata@nist.gov)  
Phone: (301) 975-2208  
FAX: (301) 926-0416

If you have technical questions relating to the data, contact:

Dr. C. J. Powell  
National Institute of Standards and Technology  
100 Bureau Dive, Stop 8370  
Gaithersburg, MD 20899-8370  
Email: [cedric.powell@nist.gov](mailto:cedric.powell@nist.gov)  
Phone: (301) 975-2534  
FAX: (301) 216-1134

Prof. Dr. A. Jablonski  
Institute of Physical Chemistry  
Polish Academy of Sciences  
ul. Kasprzaka 44/52  
01-224 Warsaw  
Poland  
Email: [ajablonski@ichf.edu.pl](mailto:ajablonski@ichf.edu.pl)  
Phone: (+48) 22-343-3331  
FAX: (+48) 22-343-3333